

# Deposition Characteristics and Microstructure of Ni60–Ni Composite Coating Produced by Supersonic Laser Deposition



Jianhua Yao, Lijing Yang, Bo Li, Qunli Zhang, and Zhihong Li

**Abstract** Supersonic laser deposition (SLD) is a newly developed coating method which combines the supersonic powder stream produced by cold spray (CS) with synchronous laser heating of the deposition zone. This article presents a study of using the SLD technique to deposit Ni60–Ni composite coatings on 45# medium-carbon steel substrate (AISI 1045). The process was investigated to identify optimum parameters such as laser power. The microstructure of coating specimens and deposition characteristics was analyzed using scanning electron microscope (SEM) and energy dispersion spectrum (EDS), respectively. The results show that the SLD technique is able to achieve a dense crack-free coating with the optimal process parameter, because Ni particles are found to have deformed largely and be evenly distributed in the coatings, which benefit releasing residual stress developed in the composite coatings during the SLD process. The cross-section thickness of the Ni60–30 wt%Ni composite coatings increased with enhanced laser power. It is also found that a Ni-rich layer is generated at the interface between the coating and substrate. This softer Ni-rich layer serves as a transition layer to accommodate the adhesion between the coating and substrate.

**Keywords** Supersonic laser deposition · Laser irradiation · Ni60–Ni composite

## 1 Introduction

Ni60 is one of the most widely used self-fluxing Ni–Cr–B–Si–C alloy powders for conventional thermal spray. Adding Si, B, Cr elements in Ni-based alloy lowers its melting point down to 1050–1080 °C and increases alloy hardness up to 58–62 HRC [1]. The enhanced alloy shows excellent resistance to wear, corrosion, high

---

J. Yao (✉) · L. Yang · B. Li · Q. Zhang · Z. Li

Research Center of Laser Processing Technology and Engineering, Zhejiang University of Technology, Hangzhou 310014, China

e-mail: [laser@zjut.edu.cn](mailto:laser@zjut.edu.cn)

Zhejiang Provincial Collaborative Innovation Center of High-End Laser Manufacturing Equipment, Hangzhou 310014, Zhejiang, China

© Springer Nature Switzerland AG 2022

S. Hinduja et al. (eds.), *Proceedings of the 38th International MATADOR Conference*, [https://doi.org/10.1007/978-3-319-64943-6\\_12](https://doi.org/10.1007/978-3-319-64943-6_12)

temperature oxidation, and combined properties over a wide range of temperature [2]. Conventional Ni60 coatings are often prepared by high velocity oxygen fuel (HVOF), plasma spray and laser cladding (LC). In thermal spray process, plasma jets or process gasses are used to melt or partially melt the particles and to accelerate the powder to impact on a prepared substrate. Ni60 coatings deposited by plasma spray have some problems: high oxides, high porosity, non-uniform microstructure, weak coating adhesion strength, low deposition efficiency, owing to unmelting powder and high thermal stress [1, 3, 4]. Laser cladding (LC) technology uses high energy density of laser beam to melt feedstock material and the surface layer of substrate to form metallurgical bonding between coating and substrate [5, 6]. Ni60 coatings deposited by laser cladding showed that oxides such as FeB, Cr<sub>3</sub>C<sub>7</sub>, Ni<sub>3</sub>Si easily concentrated at the grain boundary, the structure stress and heat stress of the coating were generated by dendritic growth during rapid solidification, and high thermal gradients were induced during rapid cooling, all of which can lead to non-uniform intermetallic compounds and the initiation of cracks [7–9]. Although metallurgical combination between coating and substrate in laser cladding can improve coating adhesion strength, element component dilution of the coating can affect the performance of the coating and form a low hardness zone [10]. In order to solve these problems and improve the properties of the coatings, cold spray which is the newest spray techniques has attracted significant attention in recent years.

Cold spray is a process whereby metal powder particles remain in solid state under the condition of deposition but are deformed plastically to form a coating by a low temperature supersonic gas stream and ballistic impingement upon a suitable substrate [11, 12]. The particles' size of metal powder ranges from 5 to 50 μm and are accelerated by means of a high-velocity jet stream which is generated through the expansion of a pressurized, preheated nitrogen or air in a converging–diverging nozzle to exceed critical plastic deformation velocity [13, 14]. Cold spray is popular in depositing low hardness, heat sensitive and oxidation sensitive materials, such as Al, Cu, Ti, 316L stainless steel, Ni-based 25 alloy, amorphous material and so on [15–19], but it is difficult to deposit high hardness particles such as Stellite6, Ni60 and metal ceramic material or prohibitively expensive to process by cold spray [20].

In order to expand the application of cold spray technology, reduce the processing costs and improve coatings' performance and quality, the idea of combining cold spray with laser technology was proposed by O'Neill [21], known as supersonic laser deposition (SLD). This combination created a potential and advanced technology to produce high performance and high quality coatings. In SLD, laser is used to heat the deposition zone and soften both substrate and powder particles to allow the formation of a coating at a much reduced impact velocity, about half of that used in cold spray [21, 22]. Because SLD reduces particle deposition temperature and critical deposition velocity, Ni60 particles can be deposited more easily with this process. In this research, Ni60–30 wt%Ni composite was deposited on 45# medium carbon steel (AISI 1045) using SLD. Different laser powers were tested to optimize the deposition process. The microstructure and coating thickness were examined using scanning electron microscopy (SEM) and energy spectrum analysis (EDS).

## 2 Experimental Methods

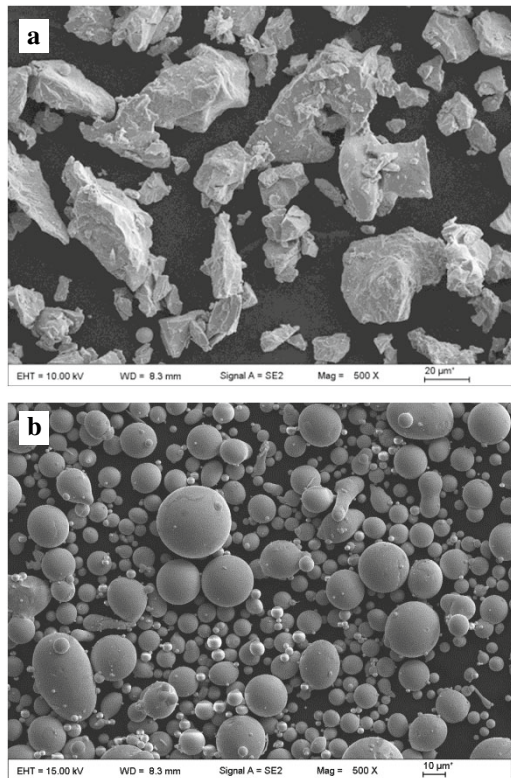
### 2.1 Composite Powder and Substrate Preparation

Commercially available pure Ni (99 wt%) powder and Ni60 alloy powder were sieved to obtain the powders having the size less than 50  $\mu\text{m}$ . Ni60 powder was prepared by gas atomization and its chemical composition is given in Table 1. The particle shape of pure Ni is irregular while that of Ni60 alloy powder is spherical, as shown in Fig. 1. The particle size distribution indicates that the powder's mean diameter is 35  $\mu\text{m}$  and 19  $\mu\text{m}$ , respectively. About 90% of Ni60 particles have a size below 26  $\mu\text{m}$ . The Ni60–30 wt%Ni composite powder was mechanically milled at a rate of 150 rpm for 2 h in alcohol environment. Stainless steel balls with 8 and 12 mm

**Table 1** Chemical composition of Ni60 alloy

Element	C	Cr	Si	B	Fe	Ni
wt. %	0.5	18	4.5	3.0	15.0	Bal

**Fig. 1** SEM morphology: **a** Ni powder (particles), **b** Ni60 powder (particles)

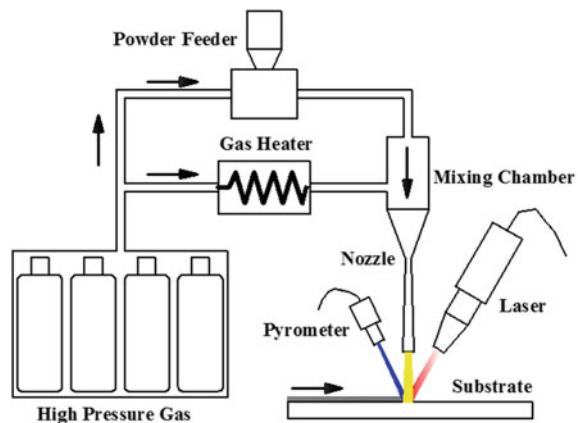


diameter were used as the grinding media, the ball-to-powder weight ratio was 35:1. The substrate is a  $100 \times 60 \times 10$  mm flat 45# medium carbon steel, whose surface was prepared by blasting using 24 Mesh  $\text{Al}_2\text{O}_3$ , then cleaning the surface of substrate by means of ultrasonic in alcohol medium.

## 2.2 Coating Preparation

The SLD system (Centre for Industrial Photonics, Institute for Manufacturing, University of Cambridge, UK, by Dr. W. O'Neill) used to prepare the Ni60-Ni composite coatings is shown schematically in Fig. 2. A high pressure (10–35 bar range) nitrogen gas supply was directly delivered to a converging nozzle. The feed-stock stream and carrier gas were mixed and passed through the nozzle where they were accelerated to supersonic speed. The high-velocity flying particles impacted a region of the substrate where a maximum power of 4 kW diode laser of 960–980 nm was synchronously irradiated. In the deposition process spraying zone and laser spot must match with each other. The temperature of deposited zone was monitored by a pyrometer whose temperature control precision was about  $\pm 2$ . Softened substrate and powder particles by means of laser allowed the formation of Ni60–30 wt%Ni composite coating at a much reduced impact velocity, which was about half of that used in cold spray. In this experiment, the nitrogen was used to accelerate the composite powder. The laser spot diameter was 5 mm, single track Ni60–30 wt%Ni composite coatings were deposited. The spraying distance was 30 mm; the traverse rate was 30 mm/s, the nitrogen temperature was 550 °C, the  $\text{N}_2$  pressure was 30 bar, the laser power varied from 2.5 to 2.8 kW with each increment of 100 W. The deposition temperatures of coatings which corresponded to the laser powers were measured by a pyrometer; the readings were 980 °C, 1000 °C, 1020 °C, 1040 °C, respectively.

**Fig. 2** Schematic showing of the SLD system



The coating specimens were sectioned and polished for microstructural analysis using SEM/EDS. The thickness of the coating layers was measured with the image analysis software of SEM. The effects of laser power on the characteristics of the coatings were studied.

### 3 Results and Discussion

The hardness of plain Ni60 coatings is about 60 HRC. It has been found that these coatings often contain cracks when produced by thermal spray or laser cladding. The SLD technology allows retaining powder particles' essential ingredients, and adding Ni particles to Ni60 can release thermal stresses to restrain cracking in the coatings. In addition, it was also observed that Ni particles were prone to concentrate at the coating/substrate interface, which improved the coating adhesion.

#### 3.1 Coating Thickness

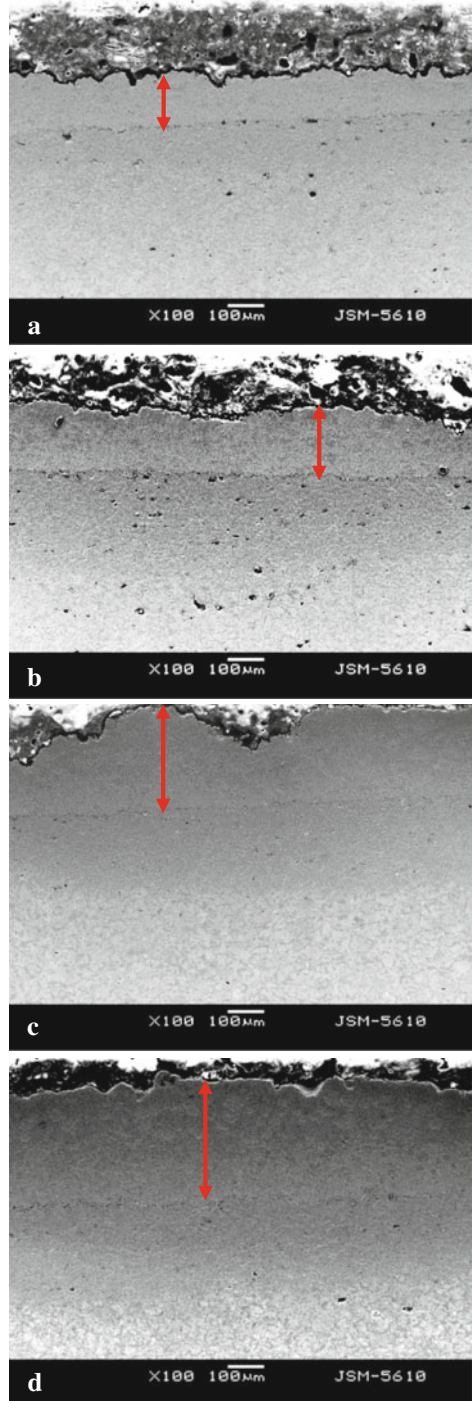
The coating thickness of the SLD-fabricated Ni60–30 wt%Ni composite coatings produced by various laser powers was evaluated with respect to peak thickness of the coatings, as shown in Fig. 3. It is observed that large tracks exist in the coatings produced with the powers of 2.5 kW and 2.8 kW, and the peak thickness of the coatings increases with enhancing laser power. Choosing three different position of single track to measure the peak thickness, the average peak values of the coatings produced with the four laser powers were  $130 \pm 6 \mu\text{m}$ ,  $192 \pm 8 \mu\text{m}$ ,  $285 \pm 11 \mu\text{m}$  and  $450 \pm 11 \mu\text{m}$ , respectively. This indicates that the deposition temperature of SLD can improve the thickness and density of the coatings effectively. With the laser power of 2.8 kW, the thickness of the coating is the most uniform.

#### 3.2 Microstructure and Cracking

##### 3.2.1 Microstructures of Ni60–30 wt%Ni Composite Coatings

The microstructures of the Ni60–30 wt%Ni composite coating specimens produced with the four laser powers were analyzed using SEM; the obtained images are presented in Fig. 4. It is observed that Ni particles are embedded uniformly in the Ni60 matrix for all the coating specimens, which implies that these particles have deformed significantly and enhanced the density of the coatings. In addition, it is found that the content and intensity of Ni particles are higher in the coating deposited at a laser powder of 2.8 kW than that of coating deposited by 2.5 kW.

**Fig. 3** SEM images of cross section of SLD Ni60–30 wt%Ni composite coatings showing peak coating thickness: **a** 2.5 kW, **b** 2.6 kW, **c** 2.7 kW, **d** 2.8 kW



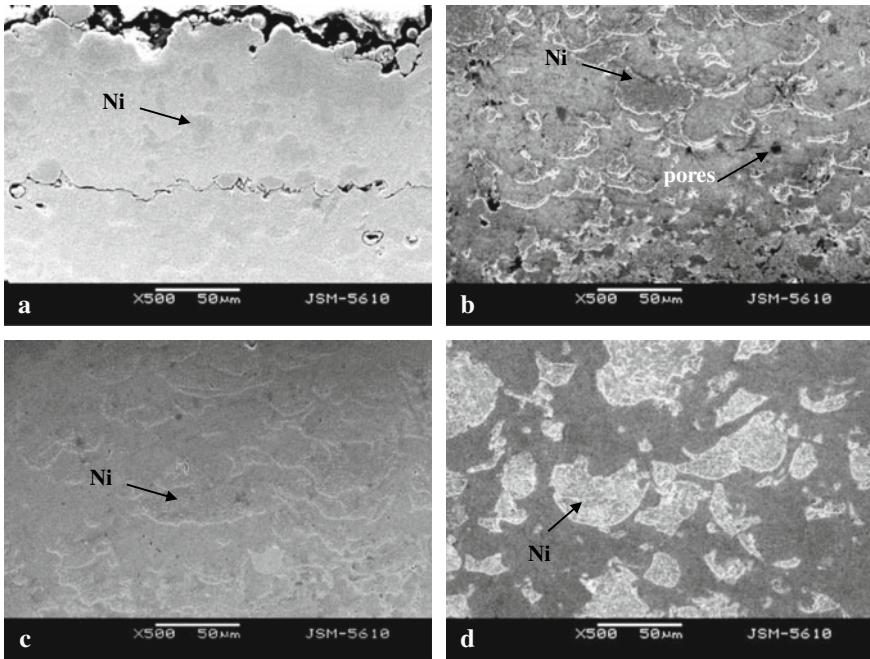
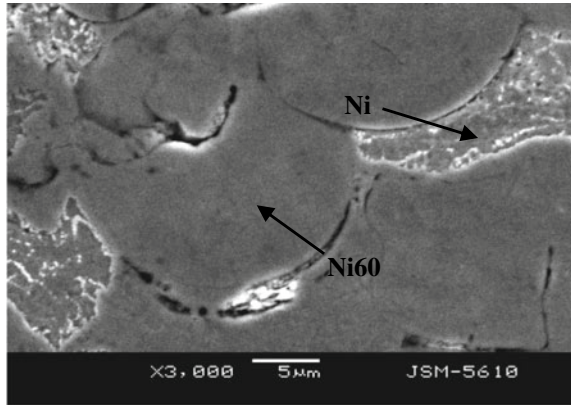


**Fig. 4** Microstructures of the Ni60–30 wt%Ni composite coatings: **a** 2.5 kW, **b** 2.6 kW, **c** 2.7 kW, **d** 2.8 kW

### 3.2.2 Cracking of Ni60–30 wt%Ni Composite Coatings

From Fig. 4 cracks are found in the coatings produced with the lower laser powers (lower deposition temperatures), but no obvious cracking is observed in the coatings deposited at the higher temperatures. This demonstrates that enhancing deposition temperature or laser power of SLD did not cause accumulation of stress, whereas it increased the coating thickness and intensity of the coating. However, Ni60 particles contained metallic compounds such as FeB,  $\text{Cr}_3\text{C}_7$ ,  $\text{Ni}_3\text{Si}$  which are easy to concentrate at grain boundaries. This usually causes cracking of coatings when produced with thermal spray or laser cladding. The higher the deposition temperature, the more the metallic compounds precipitated, thus the higher the thermal stress accumulated, leading to cracking of the coating. In the SLD process, the heat-affected zone can be reduced thus minimizing thermal stress and cracking. Moreover, pure Ni is relatively soft and Ni particles present in the coatings serve as tiny sponge particles which can release the stress of the coatings and effectively suppress cracks. As shown in Fig. 5, Ni particles deformed larger than Ni60 particles, and they are squeezed between Ni60 particles.

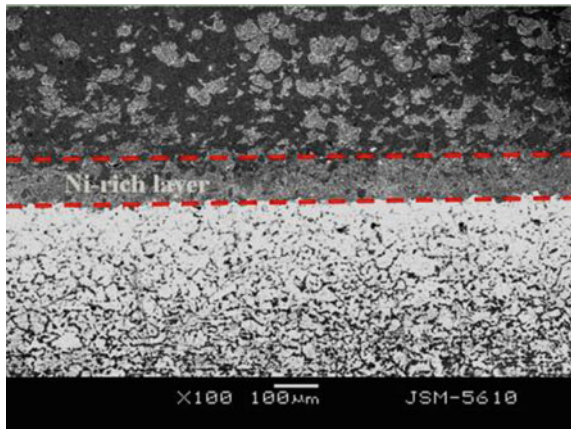
**Fig. 5** SEM image showing deformed Ni particles in the composite coating produced with 2.8 kW laser power



### 3.3 Ni-Rich Layer in the Ni60–30 wt%Ni Coatings

Observation of the fabricated Ni60–30 wt%Ni composite coating with 2.8 kW laser power discovered that Ni particles in the composite powders formed a Ni-rich layer at the coating/substrate interface. The presence of this layer in the coatings is like a sandwich, as shown in Fig. 6. The softer Ni-rich layer plays a role of transition layer for effective bonding between the hard coating and substrate. The element mapping EDS analysis confirmed the presence of the Ni-rich layer in the coatings, as shown in Fig. 7, higher Ni element concentration was found in the interfacial bond zone. Figure 7 shows the element distributions of Ni, Cr, Fe and Si in the Ni60–30 wt%Ni coating.

**Fig. 6** Ni-rich layer between coating and substrate in the Ni60–30 wt%Ni composite coating





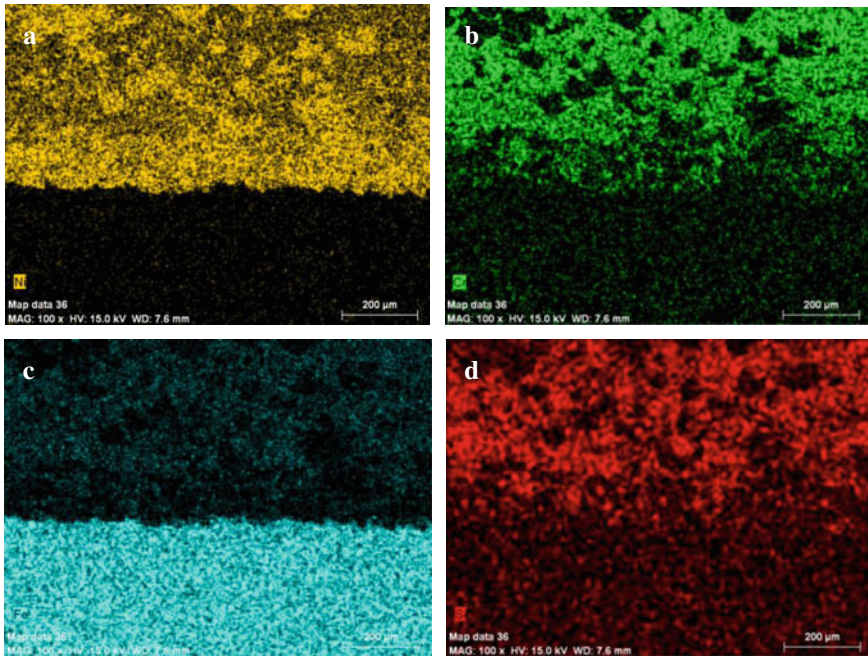


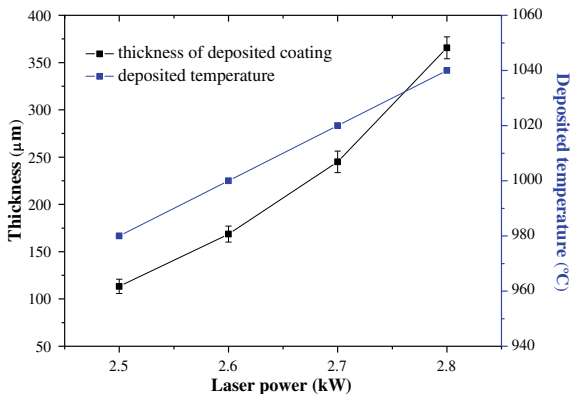
**Fig. 7** SEM/EDS mapping images of various elements in the Ni60–30 wt%Ni composite coating showing a Ni-rich layer interfacial zone: **a** Ni, **b** Cr, **c** Fe, **d** Si

### 3.4 Discussion

An analysis of the laser beam interaction with the Ni60–30 wt%Ni composite powder stream accelerated by post-heating high pressure  $N_2$  suggests that high-energy intensity of diode laser beam can quickly irradiate molecules of the gas and composite powder particles flying at a high speed. As a result, kinetic energies of the Ni60–30 wt%Ni powder particles and molecules of the gas were promoted via the convection process with the attendant effect of an increase in deposit temperature [23]. An increment in the kinetic energy of the atoms of the Ni60–30 wt%Ni particles via the conduction process translates loosening of their atomic bond energy, which then results in particle softening as their yield strengths are reduced [22]. Moreover, the laser irradiation also has a softening effect on the deposition zone and the surface of the substrate via the heat conduction process [21, 22]. All of these can enhance the deposition process of the powder particles with increased speed and deformation, which cannot be achieved by cold spray. Furthermore, appropriate deposition temperature for lower yield strength powder particles below their radiating temperature of laser beam can cause an increment in coating thickness as shown in Figs. 3 and 8.

Figure 8 presents the variations of deposition temperature and coating thickness of the composite coatings with laser power. It is known that Ni60 is of the type of self-fluxing alloy, adding Si, B, Cr elements in Ni-based alloy makes its melting

**Fig. 8** Variations of the coating thickness and deposition temperature of the Ni60–30 wt%Ni composite coating with applied laser power



point down to 1050–1080 °C [1]. Moreover, the melting point of pure Ni is higher than that of Ni60 alloy so that Ni60 particles were easier softened than Ni particles by the action of laser. The shapes of pure Ni and Ni60 alloy particles are irregular and spherical, respectively. According to the theory of gas dynamics, the gas drag coefficient of the non-spherical particles is greater than that of spherical particles. The gas force is proportional to the gas drag coefficient, as expressed by the equation below:

$$D = \frac{1}{2} \rho v_{rel}^2 A_p C_D \quad (1)$$

where  $D$  and  $\rho$  are the drag force and the density of accelerating gas, respectively;  $v_{rel}$  and  $A_p$  are the relative velocity of the gas to particle and the superficial area of particle, respectively. The studies by other researchers demonstrated that non-spherical particle could attain greater impacting velocity than spherical particle with the same process parameters, because non-spherical particle possesses larger shape form drag [24]. Therefore, it is found that Ni particles are distributed uniformly with large deformation in the Ni60 matrix, as seen in Fig. 4. These results indicated that Ni particles and Ni60 particles have different deposition cases, Ni particles uniformly distribute in composite coatings by completely deforming solid state, presented in Fig. 4.

Since the melting point of pure Ni is higher than that of Ni60 alloy, the Ni60 particles could be softened more severe than Ni particles by the laser heat. Owing to larger shape form drag of non-spherical Ni particles, the non-spherical Ni particles can attain greater impacting velocity than spherical Ni60 particles with the same process parameters. This made the Ni particles easier to deposit on the substrate than Ni60 particles. As well known, the process of spraying particles on the surface of substrate will cause plastic deformation of both materials due to particle impact and the interaction time is very short; so that almost no plastic deformation energy is lost. This provides the particles with adiabatic shear instability to deposit on the substrate. Li et al. suggested that the less the elastic limit of metallic particle, the

stronger the bonding between the coating and substrate is [25], as explained by the equation below:

$$\varepsilon_e = \frac{\varepsilon_s}{E} \quad (2)$$

where  $\varepsilon_e$ ,  $\sigma_s$  are elastic limit, yield strength and elasticity modulus, respectively. The elastic limit and hardness of pure Ni are less than those of Ni60 alloy. Therefore, Ni particles can be easier deposited on the substrate than Ni60 particles, which resulted in the Ni-rich layer at the interface of the coatings.

## 4 Conclusions

The dense, crack-free and well-bonded Ni60–30 wt%Ni composite coatings were deposited successfully on 45# medium carbon steel with a wide range of laser power or deposition temperature. The thickness of the Ni60–30 wt%Ni composite coatings increased with enhanced laser power. Microstructural examinations reveal that in the SLD process Ni particles with plastic deformation were uniformly embedded in the Ni60 matrix. The plastic deformation of Ni particles benefited releasing residual stress developed in the composite coatings during the SLD process, thus achieving crack-free and dense coatings. A Ni-rich layer formed at the interface between the coating and substrate. This softer Ni-rich layer plays a role of transition layer for the strong adhesion between the hard coating and substrate. The research results have shown that SLD is capable of depositing hard composite coating in good quality.

**Acknowledgements** The authors would like to appreciate financial supports from the National Natural Science Foundation of China (51475429), the Youth Foundation Projects of Natural Science Foundation of Zhejiang Province (LQ13E050012), and the Commonweal Technology Research Industrial Project of Zhejiang Province (2013C31012).

## References

1. Zhang XC, Xu BS, Tu ST, Xuan FZ, Wang HD, Wu YX (2008) Effect of spraying power on the microstructure and mechanical properties of supersonic plasma-sprayed Ni-based alloy coatings. *Appl Surf Sci* 254:6318–6326
2. Hong S, Wu YP, Li GY, Wang B, Gao WW, Ying GB (2013) Microstructural characteristics of high-velocity oxygen-fuel (HVOF) sprayed nickel-based alloy coating. *J Alloy Compd* 581:398–403
3. Gil L, Staia MH (2002) Influence of HVOF parameters on the corrosion resistance of NiWCrBSi coatings. *Thin Solid Films* 420:446–454
4. Kim HJ, Hwang SY, Lee CH, Juvanon P (2003) Assessment of wear performance of flame sprayed and fused Ni-based coatings. *Surf Coat Technol* 172:262–269
5. Sexton L, Lavin S, Byrne G, Kennedy A (2002) Laser cladding of aerospace materials. *J Mater Process Technol* 122:63–68

6. Vilar R (1999) Laser cladding. *J Laser Appl* 11:64–79
7. Boiciuc S, Levcovici DT (2009) Properties and application of laser cladding with Ni–Cr–B–Fe–Al ALLOY. *Metal Int* 14:49–53
8. Hemmati I, Ocelik V, De Hosson JTM (2013) Advances in laser surface engineering: tackling the cracking problem in laser-deposited Ni–Cr–B–Si–C Alloys. *Jom* 65:741–748
9. Hemmati I, Rao JC, Ocelik V, De Hosson JTM (2013) Electron Microscopy Characterization of Ni–Cr–B–Si–C Laser Deposited Coatings. *Microsc microanal* 19:120–131
10. Boiciuc S, Levcovici S, Levcovici DT, Gheorghies C (2008) Characterisation of hard coatings obtained by laser cladding process. *Metal Int.* 13:32–39
11. Alkhimov AP, Kosarev VF, Papyrin AN (1990) A method of cold gas-dynamic spraying. *Dokl Akad Nauk SSSR* 315:1062–1065
12. Kosarev VF, Klinkov SV, Alkhimov AP, Papyrin AN (2003) On some aspects of gas dynamics of the cold spray process. *J Therm Spray Technol* 12:265–281
13. Assadi H, Gartner F, Stoltenhoff T, Kreye H (2003) Bonding mechanism in cold gas spraying. *Acta Mater* 51:4379–4394
14. Stoltenhoff T, Kreye H, Richter HJ (2002) An analysis of the cold spray process and its coatings. *J Therm Spray Technol* 11:542–550
15. Ajdesztajn L, Jodoin B, Richer P, Sansoucy E, Lavernia EJ (2006) Cold gas dynamic spraying of iron-base amorphous alloy. *J Therm Spray Technol* 15:495–500
16. Li WY, Li CJ, Liao HL (2006) Effect of annealing treatment on the microstructure and properties of cold-sprayed Cu coating. *J Therm Spray Technol* 15:206–211
17. Li WY, Liao HL, Li CJ, Bang HS, Coddet C (2007) Numerical simulation of deformation behavior of Al particles impacting on Al substrate and effect of surface oxide films on interfacial bonding in cold spraying. *Appl Surf Sci* 253:5084–5091
18. Li WY, Zhang C, Guo XP, Xu JL, Li CJ, Liao HL et al (2007) Ti and Ti–6Al–4V coatings by cold spraying and microstructure modification by heat treatment. *Adv Eng Mater* 9:418–423
19. Ajdesztajn L, Jodoin B, Schoenung JM (2006) Synthesis and mechanical properties of nanocrystalline Ni coatings produced by cold gas dynamic spraying. *Surf Coat Technol* 201:1166–1172
20. Cinca N, Lopez E, Dosta S, Guilemany JM (2013) Study of stellite-6 deposition by cold gas spraying. *Surf Coat Technol* 232:891–898
21. Lupoi R, Sparkes M, Cockburn A, O’Neill W (2011) High speed titanium coatings by supersonic laser deposition. *Mater Lett* 65:3205–3207
22. Bray M, Cockburn A, O’Neill W (2009) The Laser-assisted Cold Spray process and deposit characterisation. *Surf Coat Technol* 203:2851–2857
23. Olakanmi EO, Tlotleng M, Meacock C, Pityana S, Doyoyo M (2013) Deposition mechanism and microstructure of laser-assisted cold-sprayed (LACS) Al–12 wt.%Si coatings: effects of laser power. *Jom* 65:776–783
24. Jodoin B, Ajdesztajn L, Sansoucy E, Zuniga A, Richer P, Lavernia EJ (2006) Effect of particle size, morphology, and hardness on cold gas dynamic sprayed aluminum alloy coatings. *Surf Coat Technol* 201:3422–3429
25. Li G (2007) Study and analysis on the effect of different incidence angles and materials property for intruding process in cold spraying. Dalian University of Technology